J. Astron. Space Sci. 21(3), 167–180 (2004)

HST NIC3 PHOTOMETRY OF METAL-RICH GLOBULAR CLUSTERS PALOMAR 6, LILLER 1, AND 47 TUC (NGC 104)

Jae-Woo Lee
Astrophysical Research Center for the Structure and Evolution of the Cosmos,
Department of Astronomy and Space Science, Sejong University, Seoul 143-747, Korea
E-mail: jaewoo@arcsec.sejong.ac.kr

(Received May 19, 2004; Accepted August 10, 2004)

ABSTRACT

We present HST NIC3 photometry of metal-rich globular clusters Palomar 6, Liller 1 and 47 Tuc (NGC 104). We discuss the interstellar reddening law for the HST NICMOS F110W/F160W photometric system which depends on the temperature of the source. The distance moduli and interstellar reddening values for Palomar 6 and Liller 1 are estimated by comparing the magnitudes and colors of RHB stars in the clusters with those of 47 Tuc. We obtain $(m - M)_0$ = 14.48 mag and $E(B - V)$ = 1.34 mag for Palomar 6 and $(m - M)_0$ = 15.17 mag and $E(B - V)$ = 2.50 mag for Liller 1.

Keywords: globular clusters: individual (NGC 104, Palomar 6, Liller 1) — color-magnitude diagrams — stars:horizontal branch — stars:Population II

1. INTRODUCTION

The basic parameters, such as interstellar reddening values, distance moduli, for example, of globular clusters near the Galactic center are largely unknown until recently due to the observational difficulties. Therefore we undertook an HST NIC3 photometric study of Palomar 6 and Liller 1 to derive reddening values and distance moduli of the cluster in comparison to 47 Tuc (NGC 104).

47 Tuc ($\alpha = 00^h24^m$, $\delta = -72°05'$; $l = 305.9°$, $b = -44.9°$; J2000) is a metal-rich ([Fe/H] = −0.80) globular cluster located at 7.4 kpc from the Galactic center and 4.5 kpc from the Sun (Harris 1996). A recent study revealed that it is relatively old globular cluster, 11.5 ± 0.8 Gyr (see for example, VandenBerg 2000). Palomar 6 ($\alpha = 17^h44^m$, $\delta = -16°13'$; $l = 2.1°$, $b = -1.8°$; J2000) is a globular cluster near the Galactic center. The previous photometric or spectroscopic studies of Palomar 6 suggeted that Palomar 6 is a metal-rich globular cluster with near- or super-solar metallicity. Minniti (1995) obtained [Fe/H] = −0.4 and Bica et al. (1998) obtained $Z/Z_\odot$ = −0.09 for Palomar 6 based on intermediate-resolution spectra. Lee & Carney (2002) employed JHK photometry of the cluster and derived [Fe/H] = −1.2 for Palomar 6 using the slope of red-giant branch (RGB) star. They also obtained $E(B - V)$ = 1.30 amg and $(m - M)_0$ = 14.28 mag for Palomar 6. More recently, Lee et al. (2004) obtained high-resolution infrared (IR) echelle spectra of 3 RGB stars and derived [Fe/H] = −1.0 for Palomar 6. Liller 1 ($\alpha = 17^h33^m$, $\delta = -33°23'$; l = 354.8°, $b = -0.2°$; J2000) is located at ≈ 2.6 kpc from the Galactic center (10.5 kpc from the Sun)

and nearly on the Galactic plane (Harris 1996). The previous studies of Liller 1 showed that it is a metal-rich cluster with a heavy reddening. Malkan (1981) derived the interstellar reddening and metallicity for Liller 1, $E(B-V) = 2.9$ and [Fe/H] = -0.21, based on a reddening-free metallicity index Q_{IR}. Armandroff & Zinn (1988) studied Liller 1 using the integrated spectrum at the Ca II triplet lines and obtained [Fe/H] = $+0.2 \pm 0.3$. They also determined the interstellar reddening of the cluster by measuring a interstellar band at 8621 Å, and found $E(B-V) \approx 2.7$. Frogel, Kuchinski, & Tiede (1995) obtained JHK photometry of the cluster. They derived the metallicity of the cluster [Fe/H] = $+0.25 \pm 0.30$ using the slope of the RGB and they claimed that Liller 1 is possibly the most metal-rich globular cluster in our Galaxy. They also derived $E(B-V)$= 3.0 and $(m-M)_0$ = 14.68 $\pm$ 0.23. Ortolani, Bica, & Barbuy (1996) studied VI photometry and they obtained $E(B-V)$ = 3.05 ± 0.25 by measuring the magnitude of the brightest RGB stars of the cluster, i.e., a point where the maximum curvature in $(I, V-I)$ color-magnitude diagram (CMD) of the metal-rich clusters. However, their reddening estimation depends on the distance modulus of the cluster which they adopted. Origlia et al. (1997) employed medium resolution ($\lambda/\Delta\lambda \approx 2000$) near-infrared spectra at 1.62 μm, and they found [Fe/H] = -0.29 ± 0.30. Bica et al. (1998) undertook a metallicity study of the globular clusters near the Galactic center with an expanded sample. They measured the Ca II triplet $\lambda\lambda$ 8498, 8542, and 8662 Å using intermediate resolution (5.4 Å pixel^{-1}) integrated spectra and they obtained $[Z/Z_{\odot}] = +0.08$ and $E(B-V) = 2.80$. Davidge (2000) presented JHK photometry of the cluster. He claimed that Liller 1 has a metallicity comparable to that of NGC 6528 and he obtained $E(B-V) = 3.13$. (The metallicity of NGC 6528 is not certain at present. NGC 6528 is thought to have a near solar metallicity.) Balachandran et al. (Carney 2001) obtained IR echelle spectra of Liller 1 RGB stars and their unpublished results show that Liller 1 is more metal-poor than [Fe/H] = -0.5. Origlia, Rich, & Castro (2002) also obtained IR echelle spectra of Liller 1 and found [Fe/H] = -0.3. Finally, Stephens & Frogel (2004) obtained [Fe/H] = -0.3 for Liller 1, using medium-resolution infrared K band spectra.

In this paper, we present HST NIC3 photometry of Palomar 6, Liller 1, and 47 tuc. The interstellar reddening values and distance moduli of Palomr 6 and Liller 1 related to 47 Tuc will be discussed.

2. OBSERVATIONS AND DATA REDUCTION

The observations for Palomar 6 and Liller 1 were carried out on 27 January 1998 (UT) and those for 47 Tuc were carried out on 14 January 1998 (UT) using HST NIC3 during so called the "first NIC3 Campaign." NIC3 was equipped with a 256 × 256 pixel HgCdTe array. The field of view (FOV) is 51.2 × 51.2 arcsec, which gives a scale of 0.2 arcsec/pixel (f/17.2). All the images were obtained through the F110W and F160W filters using the MULTIACCUM mode (Calzetti et al. 1999). For Palomar 6 and 47 Tuc, images from the two different locations were obtained and, for Liller 1, images from one location were obtained. For Palomar 6, the locations of the pointing were $\alpha = 17^h43^m42^s$, $\delta = -26°13'21''$ (Palomar 6-F1) and $\alpha = 17^h43^m47^s$, $\delta = -26°13'50''$ (Palomar 6-F2). For Liller 1, the location of the pointing was $\alpha = 17^h33^m23^s$ and $\delta = -33°23'41''$. For 47 Tuc, the locations of the pointing were $\alpha = 00^h24^m11^s$, $\delta = -72°05'20''$ (47 Tuc-F1) and $\alpha = 00^h24^m22^s$, $\delta = -72°06'12''$ (47 Tuc-F2). For each field, the spiral pattern dithering (SPIRAL-DITH), which produces a spiral around the first pointing, at three positions with a 4.5-pixel (= 0.9 arcsec) offset was applied to improve flat fielding, avoid bad pixels, and reduce the effect from the undersampled PSF. In Table 1 we present the journal of observations.

All images have been processed using the standard NICMOS calibration pipeline procedure (CALNICA in STSDAS/IRAF) to perform bias subtraction, bad pixel identification, dark current

Table 1. Journal of observations for HST NIC3 photometry of Palomar 6, Liller 1, and 47 Tuc.

ID	Field	Filter	Date/Time (UT Start)	t_{exp} (sec)	Sequence Name	No. Samp.
Palomar 6	F1	$F110W$	1998 Jun 27 04:30	255.95	STEP128	12
	F1	$F160W$	1998 Jun 27 04:35	223.96	STEP032	15
	F1	$F110W$	1998 Jun 27 04:40	255.95	STEP128	12
	F1	$F160W$	1998 Jun 27 04:44	223.96	STEP032	15
	F1	$F110W$	1998 Jun 27 04:49	255.95	STEP128	12
	F1	$F160W$	1998 Jun 27 04:53	223.96	STEP032	15
	F2	$F110W$	1998 Jun 27 04:59	63.96	STEP032	10
	F2	$F160W$	1998 Jun 27 05:00	63.96	STEP032	10
	F2	$F110W$	1998 Jun 27 05:02	47.96	STEP016	10
	F2	$F160W$	1998 Jun 27 05:03	47.96	STEP016	10
Liller 1	F1	$F160W$	1998 Jun 27 07:49	639.93	STEP128	15
	F1	$F110W$	1998 Jun 27 08:00	767.93	STEP128	16
	F1	$F160W$	1998 Jun 27 08:13	639.93	STEP128	15
	F1	$F160W$	1998 Jun 27 08:19	639.93	STEP128	15
	F1	$F110W$	1998 Jun 27 09:30	767.93	STEP128	16
	F1	$F110W$	1998 Jun 27 09:44	767.93	STEP128	16
47 Tuc	F1	$F110W$	1998 Jan 14 01:52	63.96	STEP032	10
	F1	$F160W$	1998 Jan 14 01:53	63.96	STEP032	10
	F1	$F110W$	1998 Jan 14 01:55	63.96	STEP032	10
	F1	$F160W$	1998 Jan 14 01:57	63.96	STEP032	10
	F1	$F110W$	1998 Jan 14 01:58	63.96	STEP032	10
	F1	$F160W$	1998 Jan 14 02:00	63.96	STEP032	10
	F1	$F110W$	1998 Jan 14 02:02	63.96	STEP032	10
	F1	$F160W$	1998 Jan 14 02:03	63.96	STEP032	10
	F2	$F110W$	1998 Jan 14 02:06	63.96	STEP032	10
	F2	$F160W$	1998 Jan 14 02:07	63.96	STEP032	10
	F2	$F110W$	1998 Jan 14 02:09	63.96	STEP032	10
	F2	$F160W$	1998 Jan 14 02:11	63.96	STEP032	10
	F2	$F110W$	1998 Jan 14 02:13	63.96	STEP032	10
	F2	$F160W$	1998 Jan 14 02:14	63.96	STEP032	10

subtraction, linearity correction, flat field correction, photometric calibration, cosmic ray identifications and correction (see below for 47 Tuc), and identifications of pixel saturation (Calzetti et al. 1999). In Figure 1, we present the final processed images of Palomar 6, Liller 1, and 47 Tuc. We compared the images of the HST NIC3 Palomar 6 field F1 and F2 with the ground-based data (Lee & Carney 2002) in Figure 2.

During the observations of 47 Tuc, the telescope pointing oscillated in a direction parallel to the V2 axis in the HST coordinate system.[1] It has been reported that this oscillation had an amplitude of $\approx$ 120 to 225 mas and a period of about 22 seconds. Thus, there were 3 full oscillations during each exposure. This telescope pointing oscillation can affect the standard NICMOS calibration pipeline procedure. Figure 3 shows how the HST NICMOS calibration pipeline procedure determines a cosmic ray hit event using the MULTIACCUM mode. The non-destructive nature of the NICMOS readout enables us to obtain intermediate pixel values at specific times during an integration. The

[1]The V2 axis is at a 45 degree angle from the instrument axes, so both the X and Y directions in the exposure have been affected.

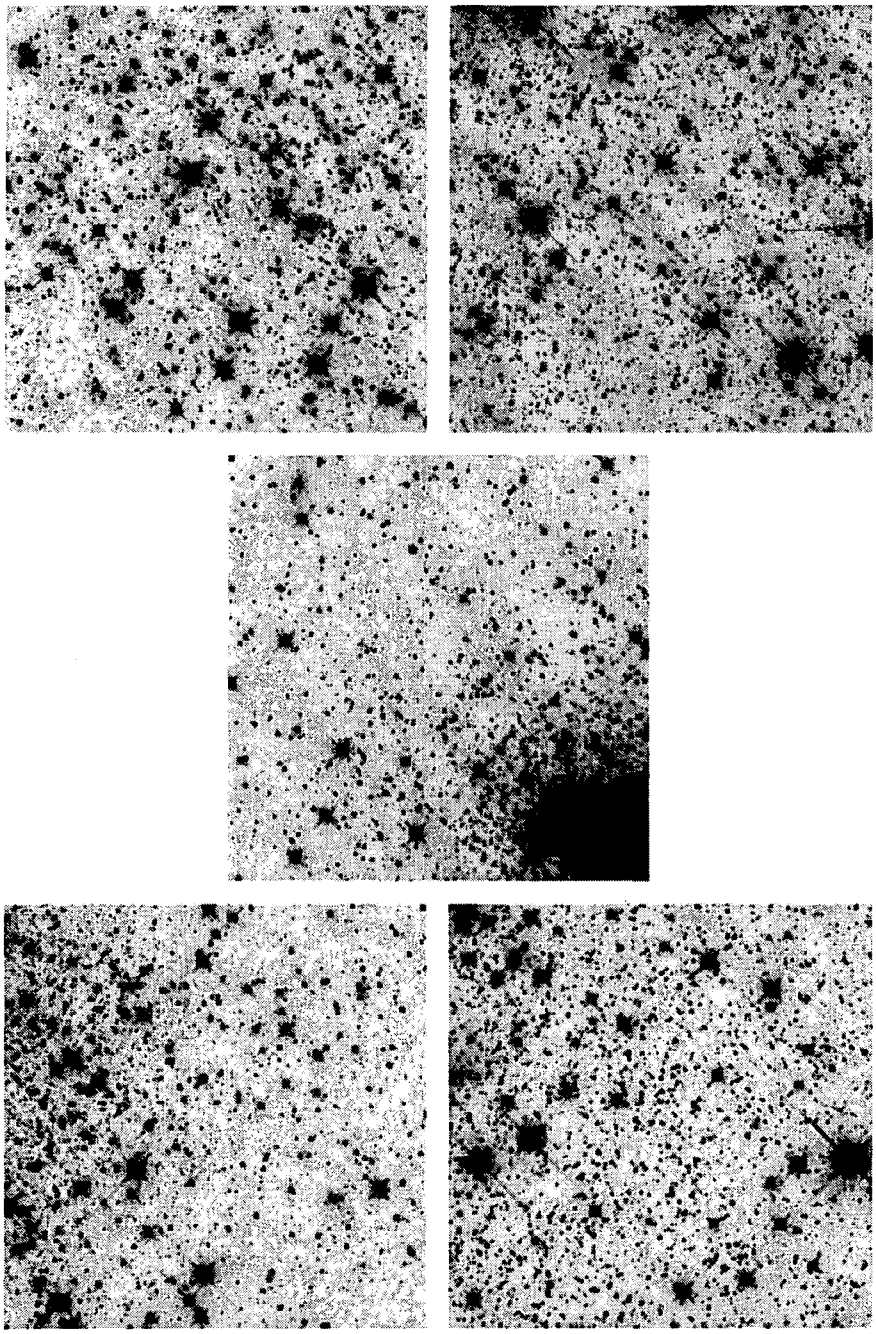

Figure 1. Final F160W images of Palomar 6 fields F1 (upper left) and F2 (upper right), Liller 1 (middle), and 47 Tuc fields F1 (lower left) and F2 (lower right).

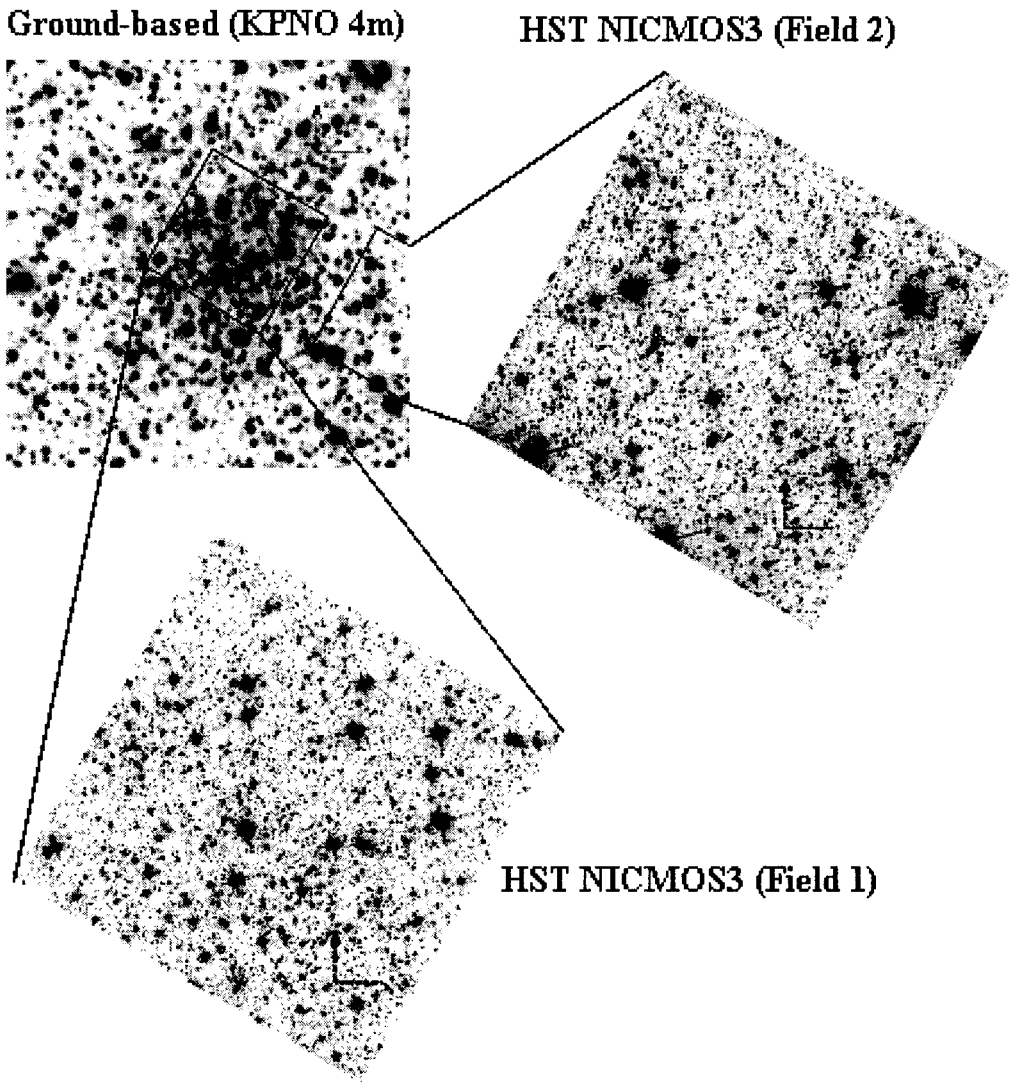

Figure 2. The positions of HST NIC3 Palomar 6-F1 and F2 in the ground-based image.

upper panel of the Figure shows a plot of the integrated signal against the integration time at a given pixel. As a cosmic ray hit event occurs, it leaves a break in slope and this distinctive feature enables us to identify a cosmic ray hit event. Once a cosmic ray hit event is identified, we can correct the observed flux at a given pixel by subtracting the contribution due to a cosmic ray hit event (see the lower panel). Although this is a very powerful observing mode provided only by NICMOS, it also causes a problem in the case of our 47 Tuc observations. As the HST pointing oscillates, the fluxes from stars also oscillate along the V2 axis and, therefore, the flux from a source, which would have been stored in a pixel if there were no oscillation in the HST pointing, will be stored in several

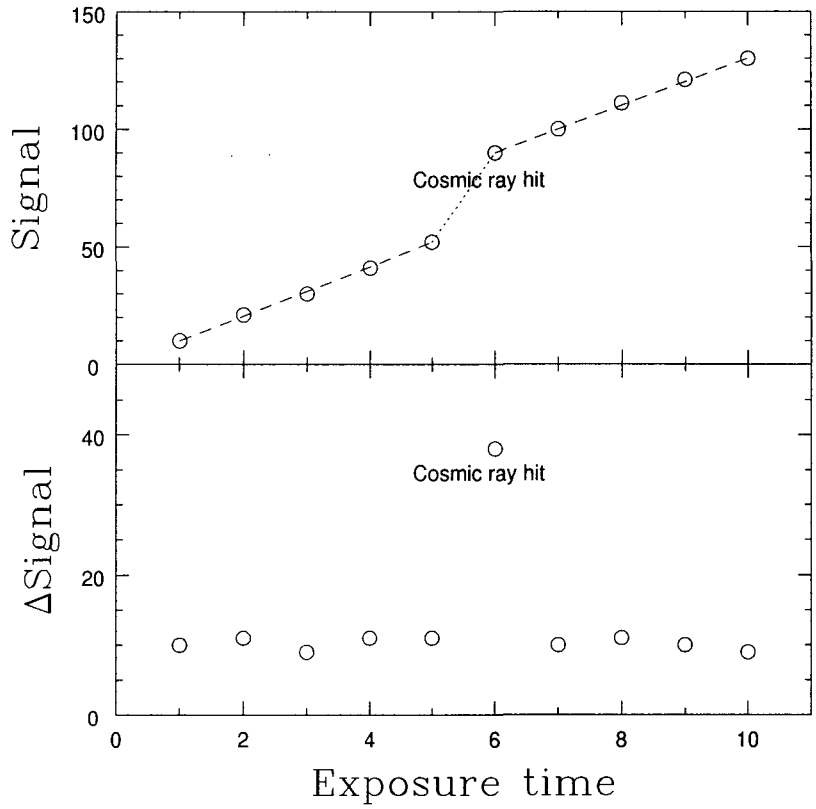

Figure 3. Schematic diagrams for the cosmic ray hit determination in the MULTIACCUM mode.

pixels. With the cosmic ray identification and correction on during our CALNICA performance, these fluctuations of the observed flux will be wrongfully identified as cosmic ray hit events. Such an example is presented in Figure 4. The Figure shows a bad pixel mask for the 47 Tuc field F1 generated during the CALNICA performance, and the most of bad pixels identified as cosmic ray hit events are located on the positions of the stars (or on the wing profile of the bright stars), indicating that the oscillation of the telescope pointing during the observations causes these misidentifications of the cosmic ray hit events. If we apply the cosmic ray correction for these images, then we lose information about the sources and we are not able to calibrate the absolute flux of the sources using

$$m_{st} = -2.5 \log (\mathrm{PHOTFLAM} \times \mathrm{CR}) - 21.1, \quad (1)$$

where PHOTFLAM is the inverse sensitivity of the instrumental setup and CR is the count rate measured in unit time. Therefore, we turned off the cosmic ray identification and correction during our CALNICA performance for the 47 Tuc fields F1 and F2 images.

PSF photometry for all images was performed with DAOPHOTII/ALLSTAR and ALLFRAME

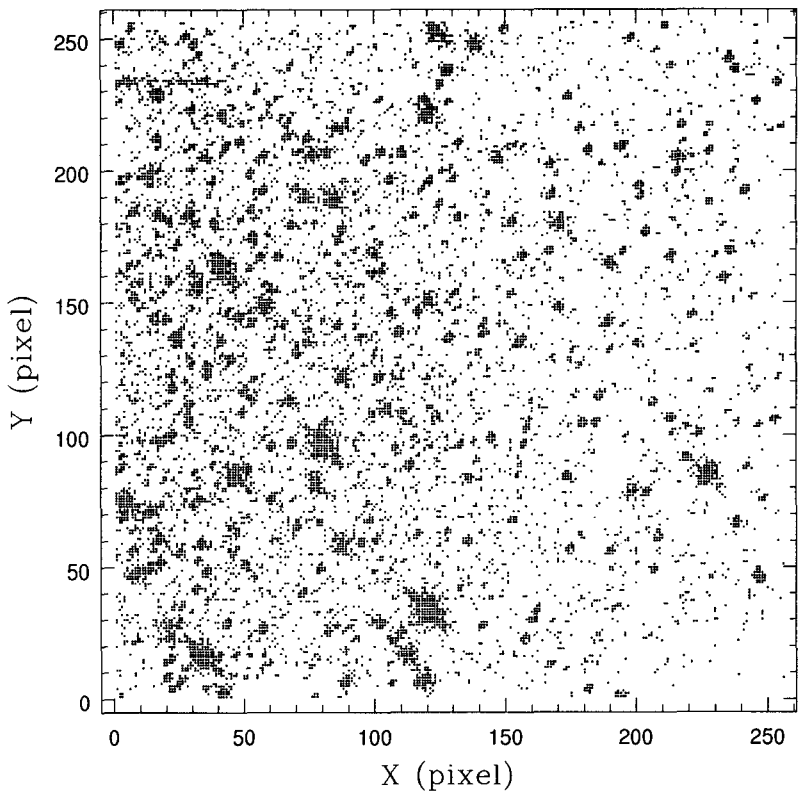

Figure 4. An example of the bad pixel mask of HST NIC3 observations for 47 Tuc during the CALNICA cosmic ray identification.

(Stetson 1987, 1994, Turner 1995) following the same procedures described in Lee et al. (2001) and our measurements were converted into the STMAG system using Equation 1.

3. RESULTS AND DISCUSSIONS

3.1 Color-Magnitude Diagrams

The CMDs for Palomar 6, Liller 1 and 47 Tuc are presented in Figures 5, 6, and 7 using the HST STMAG system. The numbers of stars measured are 2742 (Palomar 6-F1), 1961 (Palomar 6-F2), 2783 (Liller 1), 2587 (47 Tuc-F1), and 2178 (47 Tuc-F2). In the Figures, we rejected stars containing saturated pixels, hot or cold pixels, or bad pixels determined during the calibration pipeline procedure within our fitting radius in the ALLFRAME run. Also the off-cluster fields were not subtracted in our CMDs. Thus, the off-cluster field contamination is expected to be very high for Palomar 6 and Liller 1 (see for example, Figure 8 of Lee & Carney (2002) for the off-cluster field contamination

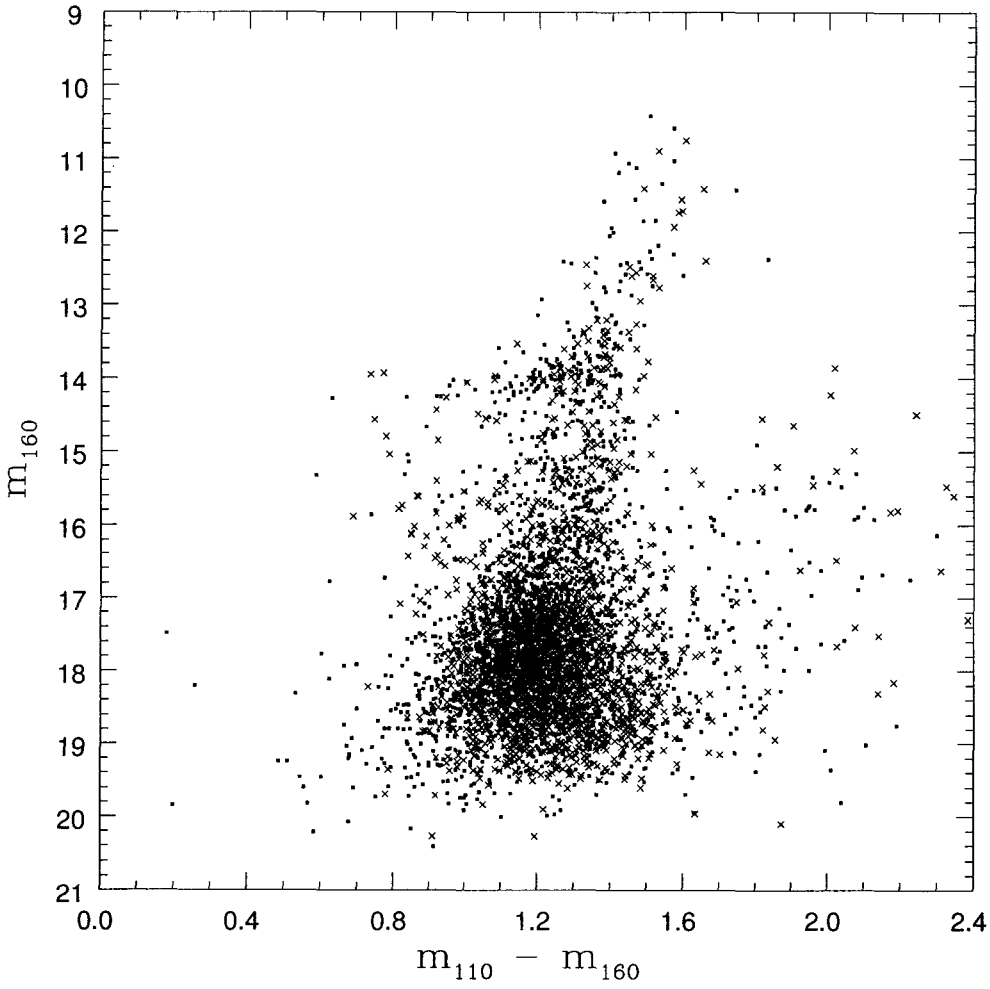

Figure 5. Composite color-magnitude diagram for Palomar 6. Dots represent the stars in the field F1 and crosses in the field F2.

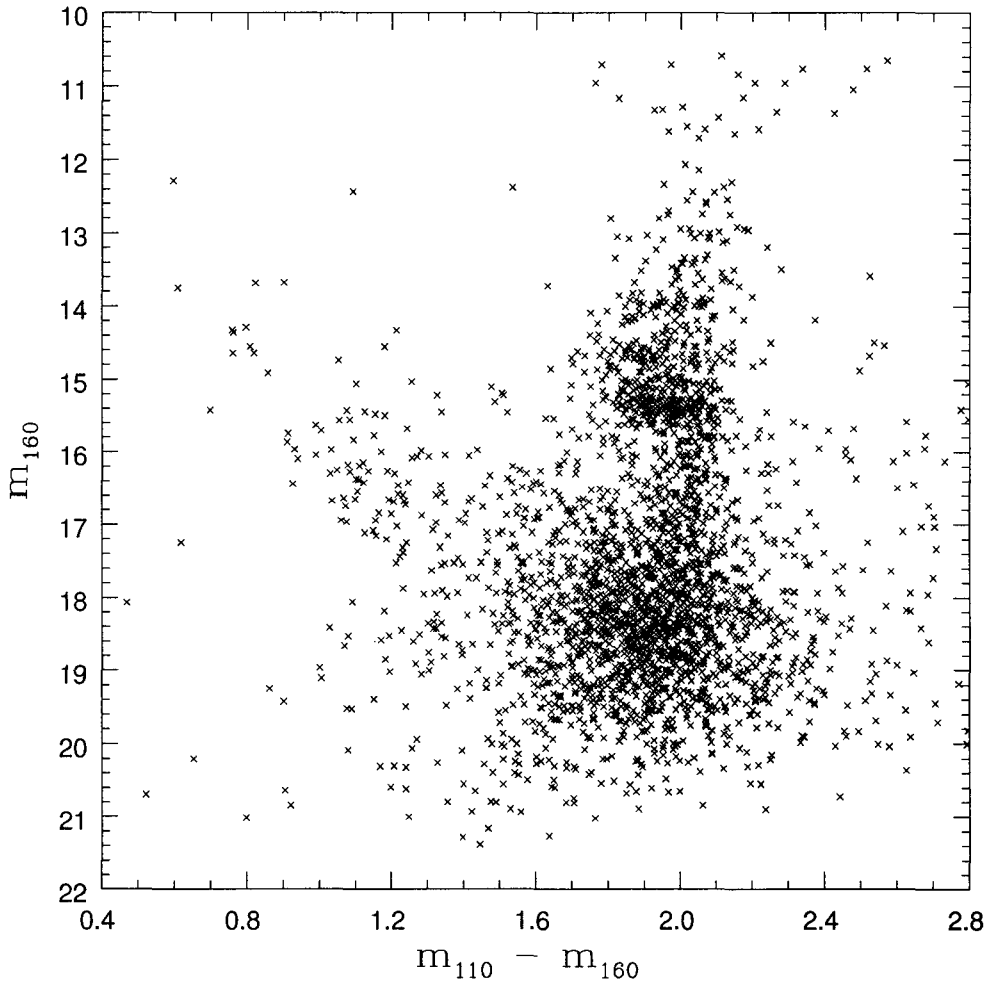

Figure 6. Composite color-magnitude diagram for Liller 1.

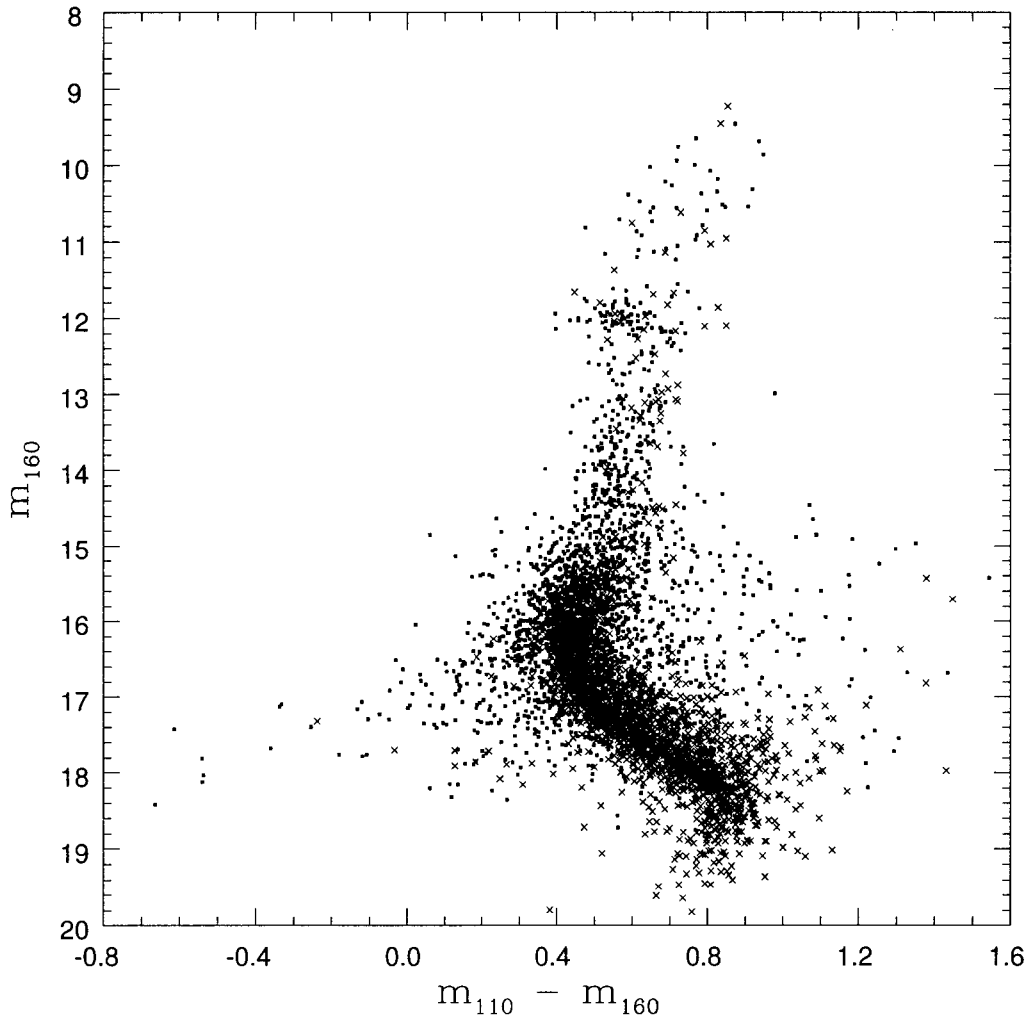

Figure 7. Composite color-magnitude diagram for 47 Tuc. Dots represent the stars in the field F1 and crosses in the field F2.

Table 2. Derived basic parameters for Palomar 6 and Liller 1.

	Palomar 6	Liller 1	Note
$E(B-V)$	1.34	2.50	
$m_{160,RHB}$	13.98	15.37	
$\Delta m_{160,0,RHB}$	1.23	1.92	1
$(m-M)_0$	14.48	15.17	2
R (kpc)	7.8	10.8	3

[1] $\Delta m_{160,0,RHB} = m_{160,RHB} - m_{160,RHB}$(47Tuc).
[2] $(m-M)_0 = \Delta m_{160,0,RHB} + 13.25$.
[3] The distance from the Sun.

toward Palomar 6).

The CMDs for Palomar 6 and Liller 1 show the red-horizontal branch (RHB) populations at $m_{160} \approx 14.0$ mag and 15.4 mag, respectively. However, our CMDs for these two clusters fail to reach below the main-sequence TO due to the under-exposure. On the other hand, the CMD for 47 Tuc shows the RHB population at $m_{160} \approx 12.0$ mag and it reaches ≈ 2 mag below the main-sequence TO, particularly in the field F2.

3.2 The interstellar reddening and the distance modulus estimates

Figure 8 shows the slopes of the RGB and the RHB magnitudes of the clusters using the methods described in Lee & Carney (2002). Note that the slope of the RGB in the $(m_{110}-m_{160}, m_{160})$ CMD breaks at near the RHB magnitude level. Also the slope of the RGB appears to be related to the interstellar reddening value as Lee et al. (2001) discussed in their Appendix A. If the three clusters have similar metallicities, then a similar slope value is expected. If Liller 1 is more metal-rich than 47 Tuc, the RGB slope[2] of Liller 1 should be smaller than that of 47 Tuc. However, the Figure suggests that the RGB slope Liller 1 is larger than that of 47 Tuc. It is thought that this discrepancy may be contributed to the differential interstellar reddening effect with the temperature of the source in the HST NICMOS F110W/F160W photometric system (see Appendix A of Lee et al. 2001). In this view, the amount of reddening suffered by lower RGB stars (i.e., hotter stars) is expected to be larger than that by the upper RGB stars (i.e., cooler stars), leading to a larger RGB slope in the observed $(m_{110}-m_{160}, m_{160})$ CMD than in the dereddened $[(m_{110}-m_{160})_0, m_{160,0}]$ CMD.

Following the similar method described in Lee & Carney (2002), we obtained the RHB magnitudes of $m_{160,RHB} = 12.00 \pm 0.14$ mag for 47 Tuc, 13.98 ± 0.20 mag for Palomar 6, and 15.37 ± 0.15 mag for Liller 1. We also derived the colors at the point where the RHB and the RGB intersect, $(m_{110}-m_{160})_{RGB,RHB} = 0.64 \pm 0.04$ mag for 47 Tuc, 1.37 ± 0.05 mag for Palomar 6, and 2.02 ± 0.05 mag for Liller 1. The error is 1 σ level. Using these colors, we examined the interstellar reddening values for Palomar 6 and Liller 1 with respect to that of 47 Tuc, $E(B-V) = 0.04$. In their Table 6, Lee et al. (2001) listed the estimated interstellar reddening law for the HST NICMOS F110W/F160W photometric system. Note that those were calculated using the synthetic spectra with [Fe/H] = -2.0, and, therefore, discrepancies may arise when applied

[2]The slope of the RGB is defined by

$$(m_{110}-m_{160}) = slope \times m_{160} + c, \quad (2)$$

and the slope usually has a negative value. Thus, the line with a zero slope is parallel to the m_{160} axis and it is more tilted to the $(m_{110}-m_{160})$ axis as the RGB slope decreases.

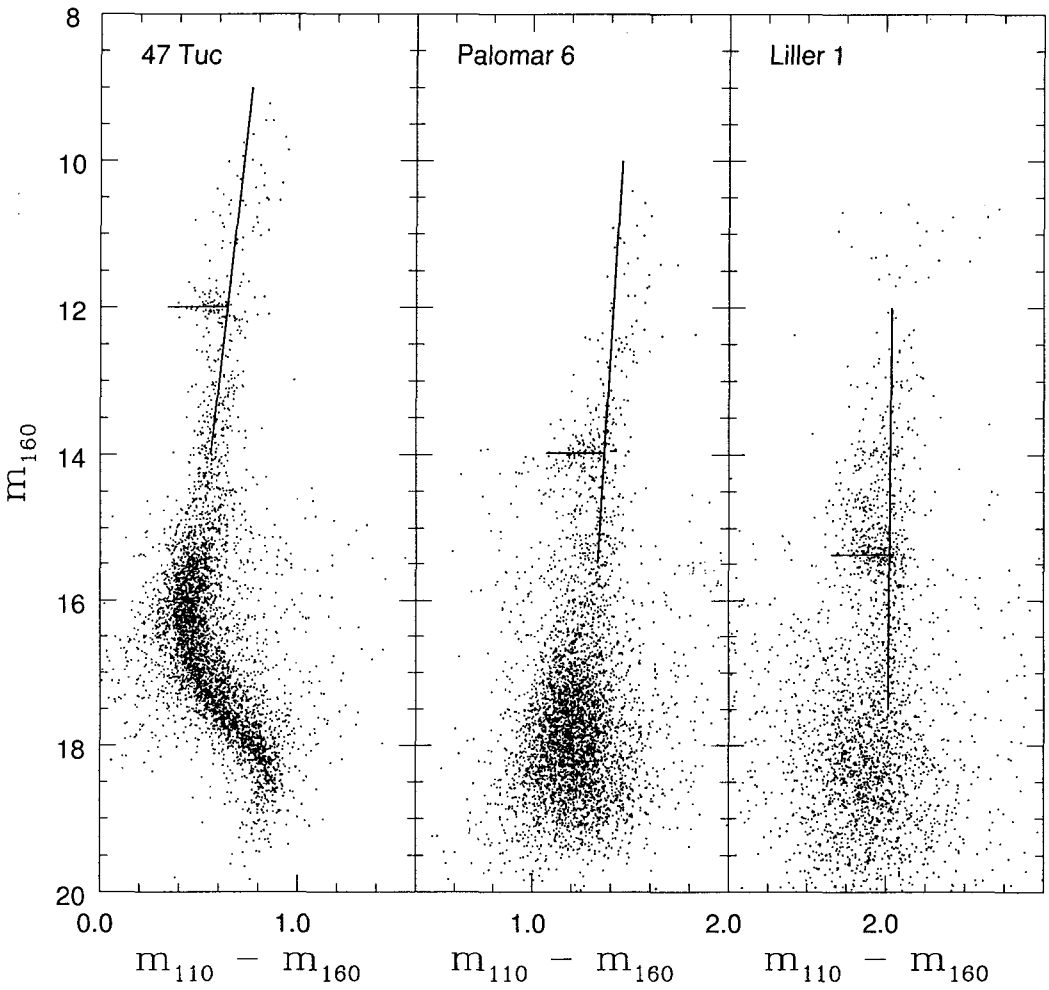

Figure 8. RGB slopes and RHB magnitudes for 47 Tuc, Palomar 6 and Liller 1.

to the metal-rich regime. Since $E(m_{110} - m_{160}) = 0.56E(B - V)$ for the RGB stars (Lee et al. 2001), $\Delta(m_{110} - m_{160})_{RGB,RHB} = 0.73$ mag for Palomar 6 with respect to 47 Tuc corresponds to $\Delta E(B - V) = 1.30$ mag and $\Delta(m_{110} - m_{160})_{RGB,RHB} = 1.38$ mag for Liller 1 corresponds to $\Delta E(B - V) = 2.46$ mag. Our interstellar reddening value $E(B - V) = 1.34$ mag for Palomar 6 agrees well with our previous estimate $E(B - V) = 1.30$ mag and those by others, ranging from $E(B - V) = 1.25$ to 1.40 mag. However, our $E(B - V) = 2.50$ mag for Liller 1 is about 0.2 - 0.6 mag smaller than the previous estimates, which range from $E(B - V) = 2.70$ mag to 3.13 mag. We also derived the distance moduli for Palomar 6 and Liller 1 by comparing their RHB magnitudes with respect to that of 47 Tuc. During our calculations, we adopt $A_{160} = 0.59E(B - V)$, and we used our interstellar reddening values $E(B-V) = 1.34$ mag for Palomar 6 and 2.50 mag for Liller 1. The distance modulus for Palomar 6 is 14.48 mag and is 0.20 mag larger than that of Lee & Carney (2002), $(m - M)_0 = 14.28$ mag, and subsequently the distance from the Sun becomes ≈ 0.6 kpc larger. Our distance modulus for Liller 1 is 15.17 mag and is 0.5 mag larger than that of Frogel et al. (1995), who obtained 14.68 mag for Liller 1. We list the results in Table 2.

4. CONCLUSIONS

In this paper, we discussed the HST NIC3 photometry of Palomar 6, Liller 1 and 47 Tuc. Our primary goal was to obtain deep IR photometry below the MSTO of the clusters, so that we can compare ages between the clusters. Since our integration times were too short, our photometric measurements failed to reach below the MSTO for Palomar 6 and Liller 1. Thus, very unfortunately, we could not estimate the ages of Palomar 6 and Liller 1.

We confirmed the previous result that the interstellar reddening law for the HST NICMOS F110W/F160W photometric system depends on the temperature of the source in comparison of the RGB slopes of Palomar 6, Liller 1 and 47 Tuc as Lee et al. (2001) discussed.

Our distance modulus estimate for Palomar 6 is ≈ 0.20 mag larger than that of Lee & Carney (2002) based on the ground-based observations, and consequently, the distance from the Sun is $\approx$ 0.6 kpc larger than the previous estimate. Our distance modulus for Liller 1 is ≈ 0.5 mag larger than that of Frogel et al. (1995).

ACKNOWLEDGEMENTS: Support for this work was provided by the Korea Science and Engineering Foundation (KOSEF) to the Astrophysical Research Center for the Structure and Evolution of the Cosmos (ARCSEC).

REFERENCES

Armandroff, T. E., & Zinn, R. 1988, AJ, 96, 92

Bica, E., Claria, J. J., Piatti, A. E., & Bonatto, C. 1998, A&AS, 131, 483

Calzetti et al. 1999, NICMOS Instrument Handbook (Baltimore: STScI)

Carney, B. W. 2001, Star Clusters, Saas-Fee Advanced Course 28. Lecture Notes 1998, Swiss Society for Astrophysics and Astronomy., eds. L. Labhardt & B. Binggeli (Berlin: Springer-Verlag)

Davidge, T. J. 2000, ApJS, 126, 105

Frogel, J. A., Kuchinski, L. E., & Tiede, G. P. 1995, AJ, 109, 1154

Harris, W. E. 1996, AJ, 112, 1487

Lee, J. -W., & Carney, B. W. 2002, AJ, 123, 3305

Lee, J. -W., Carney, B. W., & Balachandran, S. 2004, AJ in press

Lee, J. -W., Carney, B. W., Fullton, L. K., & Stetson, P. B. 2001, AJ, 122, 3136
Malkan, M. A. 1981, in IAU Colloq. 68: Astrophysical Parameters for Globular Clusters, ed, A. G D. Philip (Schenectady: L. Davis Press Inc.), p.533
Minniti, D. 1995, A&A, 303, 468
Origlia, L., Rich, R. M., & Castro, S. 2002, AJ, 123, 1559
Origlia, L., Ferraro, F. R., Fusi Pecci, F., & Oliva, E. 1997, A&A, 321, 859
Ortolani, S., Bica, E., & Barbuy, B. 1996, A&A, 306, 134
Stephens, A. W., & Frogel, J. A. 2004, AJ, 127, 925
Stetson, P. B. 1987, PASP, 99, 191
Stetson, P. B. 1994, PASP, 106, 250
Turner, A. M. 1995, Cooking with ALLFRAME (Victoria: Dominion Astrophys. Obs.)
VandenBerg, D. A., 2000, ApJS, 129, 315